

Adsorption characteristics of propan-2-ol vapours on activated carbon Sorbonorit 4 in electrothermal temperature swing adsorption process

D. Downarowicz

Received: 9 September 2014/Revised: 22 December 2014/Accepted: 12 January 2015/Published online: 23 January 2015
© The Author(s) 2015. This article is published with open access at Springerlink.com

Abstract Adsorption characteristics of propan-2-ol on Sorbonorit 4 activated carbon were determined using the breakthrough curve tests in a cyclic electrothermal temperature swing adsorption process. Maximum adsorption capacity, breakthrough time, throughput ratio and length of unused bed were also evaluated. As a result of multiple regeneration, the adsorption capacity of Sorbonorit 4 increased. Electrothermally-induced changes in the internal structure of Sorbonorit 4 and in the chemical composition of its surface were assessed based on adsorption equilibrium measurements by the gravimetric method and X-ray photoelectron spectroscopy (XPS). Three samples of virgin, direct resistively heated and electrothermally regenerated Sorbonorit 4 were used. The structural characteristics of activated carbon show that that fresh and direct resistive heated Sorbonorit 4 has a bimodal structure. Regenerated activated carbon contains one fraction of micropores. XPS analysis revealed that the same hydroxyl, carbonyl and carboxyl groups were found on the surface of all Sorbonorit 4 samples, albeit in different volume ratios. Regenerated Sorbonorit 4 has higher adsorption capacity than pure adsorbent while resistively heated Sorbonorit 4 displays lower adsorption efficiency.

Keywords Adsorption · Activated carbon · Electrothermal regeneration · IPA · Thomas model · XPS

1 Introduction

Activated carbon is widely used in adsorption systems for gas separation and air purification with recovery of valuable compounds. It is also used as catalyst support in chemical processes (Rodriguez-Reinoso 1998). Adsorption systems enable recovery of volatile organic compounds (VOC) emitted from small emission sources (Coss and Cha 2000), including propan-2-ol (IPA). VOC recovery is generally conducted in columns with adsorbent fixed-beds in temperature swing adsorption (TSA) systems. Activated carbon adsorption capacity gradually deteriorates during the process which inhibits its purification efficiency. Once the boundary VOC concentration has been reached in a purified gas, the waste adsorbent is thermal regenerated in situ. However, TSA is a long-lasting and energy-consuming process and desorption produces very dilute gas mixtures that require further treatment. The porous structure of regenerated activated carbon may be changed, resulting in reduction of its adsorption capacity in successive adsorption cycles (Ania et al. 2004).

Electrothermal regeneration offers a real alternative to thermal methods. The spent adsorbent is heated following direct conversion of electromagnetic energy into thermal energy which occurs simultaneously throughout the whole bed volume. The method benefits from much shorter heating time, better control of the process, high safety level, process automation and reduction of equipment size (Petkovska et al. 2007). Electrothermal methods can be used to regenerate various types of activated carbon, including granular activated carbon, activated carbon fiber cloth (ACFC) or activated carbon monolith (Luo et al. 2006). Regeneration is typically conducted using the direct resistance heating method (Hashisho et al. 2009; Grande et al. 2009; Downarowicz and Gabruś 2008) or the

D. Downarowicz (✉)
Faculty of Chemical Technology and Engineering, West
Pomeranian University of Technology, Szczecin, Al. Piastów 42,
71-065 Szczecin, Poland
e-mail: ddownar@zut.edu.pl

microwave method (Hashisho et al. 2005). The former uses Joule effect of direct flowing electric current. A regenerated adsorbent bed is placed between a pair of electrodes while voltage is applied to them. The current flows through aromatic parts of pseudo-graphitic domains and π -electrons are voltage carriers (Celzard et al. 2000). The method requires activated carbon to have adequate electric conductivity (Hashisho et al. 2009). Microwave heating is the effect of absorption of microwave energy by the adsorbent in an electromagnetic field. The dielectric properties of an adsorbent–adsorbate system play a decisive role in the method's effectiveness (Jou et al. 2010). The method is also used to modify the surface chemistry of active carbons (Li and Li 2012; Figueiredo et al. 1999; Shen et al. 2008).

The literature contains few reports on the effect of resistive heating on adsorption properties of activated carbon, and particularly its granulated type. However, it is essential to understand the nature of the process in order to be able to properly design ETSA recovery systems which should be able to offer better efficiency of VOC recovery to classical TSA systems. The aim of the present study was to assess the influence of direct resistive heating on the adsorption characteristics of Sorbonorit 4 activated carbon used for IPA vapour adsorption in a cyclic ETSA process.

2 Experimental section

2.1 Materials

Activated carbon Sorbonorit 4 was purchased from Norit Americas Inc., Netherlands. It is a steam activated extruded carbon with cylindrical particles with diameter of 3.8 mm and length of 5–13 mm (Gu et al. 1999). Owing to its favourable adsorption properties (BET surface area 1,400 m²/g), it is used in solvent recovery applications. This type of activated carbon was chosen out of other commercial carbon adsorbents owing to its electrical properties enabling an effective use of the resistive heating method (Paderewski and Downarowicz 2002). Prior to tests virgin Sorbonorit 4 was dried at 378 K for 24 h and stored in a desiccator until used. Propan-2-ol (IPA) with analytical purity of 99.7 % purchased from Chempur (Poland) was used as the adsorbate. The basic properties of IPA are presented in Table 1.

It is a colourless, flammable liquid with a strong odour. The lower explosive limit for IPA is 2.0 % (Yaws 2003).

The alcohol is widely used as a washing, cleaning and dehydrating agent.

2.2 Methods

2.2.1 Adsorption of IPA vapours in ETSA system

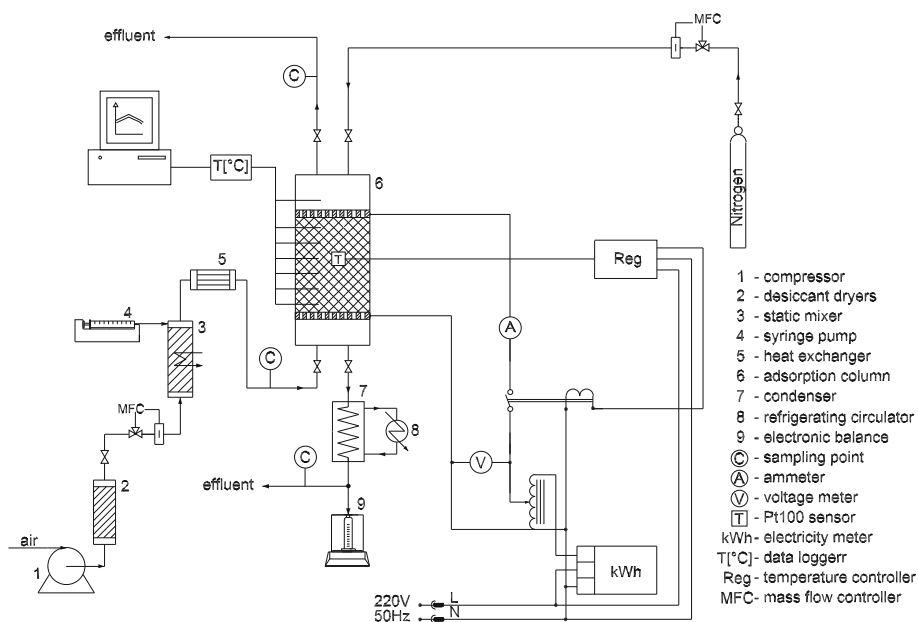
Figure 1 presents the experimental set-up of ETSA system for IPA vapour capture from air. The process was conducted in a glass adsorption column (0.055 m i.d.) with Sorbonorit 4 fixed-bed with the mass of 0.26 kg and height of 0.27 m. Voltage was applied across copper, profiled electrodes placed at both ends of the bed. Their construction was discussed at length elsewhere (Downarowicz and Nastaj 2002). The bed temperature during ETSA process was monitored by type K thermocouples mounted horizontally along vertical axis of the adsorption column. The thermocouples are connected to a temperature data logger (ACR Systems Inc., Smart Reader Plus 6) controlled by a personal computer. The ambient temperature is also monitored.

The ETSA process cycle consists of adsorption, electrothermal regeneration and cooling steps. Gas mixture for adsorption stage of ETSA process was generated by mixing IPA with purified air. Compressed air was passed through desiccant dryers (Kaeser, model DC 1.5–7.5) in order to minimize the effect of moisture during adsorption process. Dried air stream passed through the organic vapour generator (static mixer) while liquid IPA was injected into the gas stream using a hypodermic needle and a syringe pump (KD Scientific, model 100). The air flow rate was measured and controlled by a mass flow controller (Aalborg, model GFC 47). The resulting gas–vapour mixture was passed through a cylindrical adsorption column. The cleaned gas was then vented to the atmosphere. Inlet and outlet IPA concentrations were measured using a gas chromatograph with a flame ionization detector. The superficial gas velocity based on an empty column was 0.15–0.25 m/s. During adsorption step the breakthrough curve (BTC) tests were performed. All experiments were conducted at ambient laboratory temperature (295–298 K). In the BTC tests, a IPA-laden air stream with specified concentrations ranging from 5 to 20 g/m³ was passed through the adsorption bed until the exhaust stream reached a particular breakthrough concentration. Some adsorption cycles were conducted until full bed saturation has been reached, indicated by a stable concentration at the column outlet. Only full BTC curves were analysed.

Table 1 Physical-chemical properties of IPA at 293 K (Yaws 2003)

Molecular formula	Molecular weight (g mol ⁻¹)	Boiling point (K)	Saturation preussre (Pa)	Liquid molar volume (cm ³ mol ⁻¹)	Dipole moment (D)
C ₃ H ₈ O	60.096	355.5	4451	76.36	1.67

Fig. 1 Experimental set-up for ETSA process



After completion of each breakthrough test, the spent adsorbent was electrothermally regenerated using the direct resistive heating method. The system was fed from the 220 V, 50 Hz mains supply via a variable-voltage transformer applied to regulate voltage. The voltage was kept constant during regeneration, with electric current intensity depending on the fixed bed's electrical resistance. The temperature of activated carbon bed in adsorption column was controlled by means of a Pt 100 sensor coupled with a thermoregulator and a contactor which caused switch on/off of electrodes voltage. The power fed to the bed is also regulated according to feedback obtained via the Pt 100 sensor. The heat power was regulated to achieve a desired mean bed temperature, which corresponds to the thermoregulator set point.

The electrothermal desorption experiments were performed in the following invariability range of operating parameters: voltage 25–30 V, nitrogen flow 0.1–0.2 m³/h and the temperature set point 403–423 K. The nitrogen flow during regeneration was counter-current to the air flow direction during adsorption. The concentrated gas-desorbed vapour mixer from the adsorber was directed to a condenser where the IPA vapours were separated from the inert gas. Desorption duration in different ETSA cycles varied between 1.5 and 3 h. After cooling down to room temperature, regenerated activated carbon was used again for IPA vapours adsorption. A sample of activated carbon (S4-reg sample) was taken after 60 adsorption cycles of ETSA process.

2.2.2 Direct resistive heating of virgin carbon

Fresh Sorbonorit 4 was resistively heated up to 423 K and then cooled down to room temperature. Resistive heating

was performed in a glass adsorption column (0.033 m i.d.) with a fixed-bed, 0.095 m in height. The column was an additional element of electrothermal regeneration section of ETSA system elaborated on in the previous paragraph. Resistive heating was conducted in inert atmosphere (nitrogen flow 0.18 m³/h), under the voltage of 20–30 V.

A sample of activated carbon (S4-ohm sample) was taken for further analysis after 8 cycles of the process.

2.2.3 IPA adsorption isotherm measurements

The measurements of IPA vapour adsorption isotherms on Sorbonorit 4 activated carbon samples were conducted using intelligent gravimetric analyser IGA-002 supplied by Hiden Isochema LTD (Warrington, United Kingdom). The statistic gravimetric method was used. Analyser IGA-002 is fitted with a sensitive microbalance with a resolution of 0.1 µg and uncertainty of ±1 µg. The balance and pressure control system were fully thermostated to 0.2 K to eliminate changes in the external environment. A sample of activated carbon with a mass of ca. 80 mg was placed in the thermostated reactor chamber with accurate temperature control (±0.1 K). The IPA liquid used to generate the vapour was placed in a thermostated reservoir at 328 K. Prior to isotherm measurements the Sorbonorit 4 sample was outgassed to constant weight at a high vacuum level (10⁻⁶ Pa) at 393 K for 2h.

IPA adsorption isotherm measurements were conducted at 293 and 298 K for different pressure set points in the relative pressure range of 0.001–0.8. Adsorption capacity of activated carbon was calculated for all isotherms as the ratio of adsorbed IPA and the weight of the adsorbent

sample after degassing. A comprehensive description of the methodology of isotherm determination with IGA-002 is presented elsewhere (Fletcher et al. 2006; Nastaj and Aleksandrak 2013).

2.2.4 X-ray photoelectron spectroscopy

X-ray photoelectron spectroscopy (XPS), a surface technique in which the electron binding energies of atoms on the surface are used to determine the elemental composition and chemical states of samples, was used to determine the chemistry of Sorbonorit 4 sample surface. The XPS measurements were performed with XPS PHI 5000 VersaProbe (ULVAC-PHI, Japan/USA) using Al monochromatic X-ray radiation (15 kV and 25 W). XPS analysis was conducted at a high vacuum level (UHV) (the base pressure inside the analysis chamber of 10^{-8} to 10^{-9} mbar). One unbroken granule of each type of activated carbon was selected for analysis. The analyser was rastered on an area of $100 \mu\text{m} \times 100 \mu\text{m}$ at the photoelectron take off angle of 45° . Wide scan spectra in the binding energy range of 0–1400 eV were taken with 0.4 eV step intervals while spectra of specific regions (C1s, O1s) were measured with 0.1 eV step intervals. The spectra were analysed and processed using CasaXPS software.

3 Results and discussion

3.1 Breakthrough curve test results

Breakthrough curve (BTC) tests were conducted at ambient temperature (295–298 K) in the following conditions: inlet concentration of IPA vapours in air stream $C_0 = 5\text{--}20 \text{ g/m}^3$, gas flow rate $1.3\text{--}2.1 \text{ m}^3/\text{h}$ (superficial gas velocity $0.15\text{--}0.25 \text{ m/s}$). BTC shows the change in IPA vapour relative concentration (C/C_0) at the column outlet with adsorption time.

Figure 2 presents breakthrough curves for various feed concentrations at constant gas velocity $0.16 \pm 0.01 \text{ m/s}$ (flow rate $1.4 \pm 0.5 \text{ m}^3/\text{h}$). In cycle C1, adsorption was conducted on virgin activated carbon. Sorbonorit 4 regenerated with direct resistive method was used in other cycles. Prior to measurements of ETSA cyclic adsorption, the adsorbent was initially heated to 423 K under nitrogen and then cooled to ambient temperature. Finally, resistive heating characteristics were determined for pure adsorbent bed (Downarowicz and Nastaj 2002). As shown in Fig. 2, the higher the inlet concentration of adsorbate, the faster the breakthrough and the steeper its slope on the breakthrough curve. Figure 3 depicts differences in breakthrough time for adsorption cycles with inlet concentration of $12.3 \pm 0.5 \text{ g/m}^3$, and gas velocity of $0.19\text{--}0.24 \text{ m/s}$.

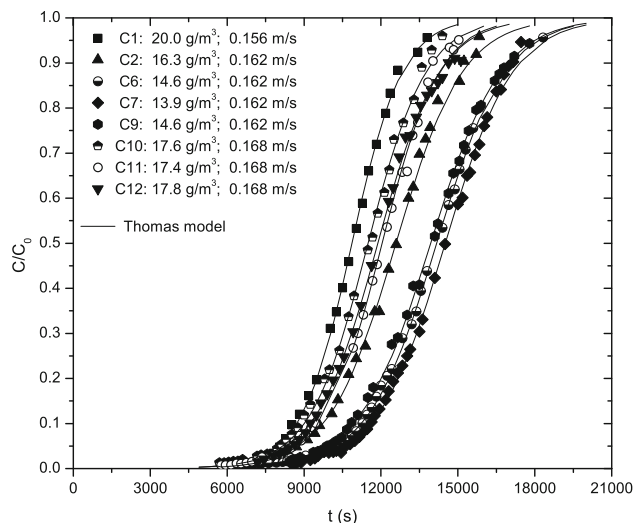


Fig. 2 Breakthrough curves at constant gas flow rate

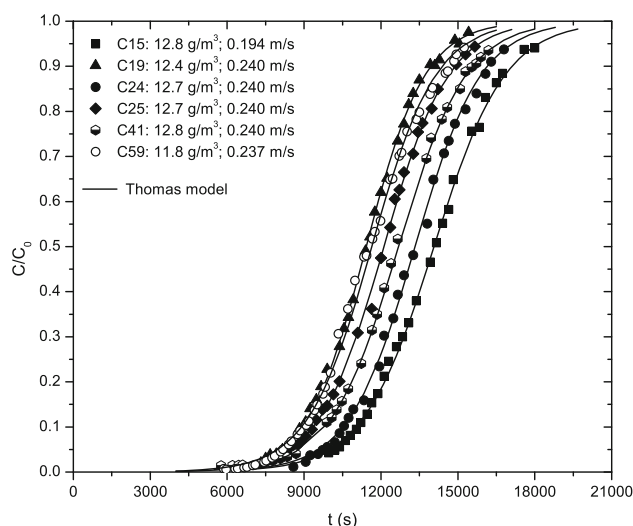


Fig. 3 Breakthrough curves at constant feed concentration

In a cyclic ETSA process, bed's useful service life at adsorption stage depends on inlet concentration, gas flow velocity and the degree of carbon regeneration. Too low adsorbent regeneration efficiency in a given ETSA cycle lowers adsorption duration in a successive cycle, as evidenced by shifted breakthrough curves in Figs. 2 and 3 determined for the same gas flow and inlet concentration value in BTC tests. Carbon regeneration efficiency depends on operating conditions at electrothermal desorption stage (temperature, voltage, nitrogen flow rate). Efficiency increases with increasing values of voltage, temperature and process duration (Downarowicz and Gabruś 2008). The bed temperature during the IPA desorption was the most homogenous when the regenerated activated carbon was fully saturated. The temperature and heating power profiles

of the electrothermal process were discussed elsewhere (Downarowicz 2006).

The breakthrough curves were characterized with following parameters: breakthrough time ($t_{5\%}$), throughput ratio (TPR) and length of unused bed (LUB). Breakthrough time denoted $t_{5\%}$ is defined as time when outlet concentration was 5 % of inlet concentration. TPR characterises the slope of the breakthrough curve and is defined as (Sullivan et al. 2004):

$$TPR = \frac{t_{5\%}}{t_{50\%}} \tag{1}$$

where $t_{50\%}$ is stoichiometric breakthrough time (time when the outlet concentration was 50 % of the inlet concentration).

Higher TPRs indicate a steeper BTC, where mass transfer limitations become less important.

LUB value determines how many per cent of adsorption capacity is not utilized at 5 % breakthrough time due to the length of the adsorption zone within the fixed-bed (Sullivan et al. 2004):

$$LUB = \left(1 - \frac{m_{5\%}}{m_{100\%}}\right) \tag{2}$$

where $m_{5\%}$ is mass of adsorbate in the fixed-bed at 5 % breakthrough time and $m_{100\%}$ mass of adsorbate in the adsorber when the adsorbent is saturated (full breakthrough).

The BTC parameter values listed in Table 2. The values of LUB and TPR are in the acceptable range of LUB values ($LUB \leq 0.3$) and TPR values ($TPR \geq 0.7$) for VOC vapour adsorption in electrothermal swing adsorption systems. The maximum LUB value for adsorption on granulated activated carbon can reach 0.5 (Sullivan et al. 2004).

Table 2 reveals that in adsorption cycles with superficial gas velocity below 0.17 m/s LUB values are generally lower. Consequently, at breakthrough time $t_{5\%}$, the unused length of bed was shorter.

The mass of IPA adsorbed during adsorption cycle was calculated from the area above the breakthrough curve at the column outlet (Ramirez et al. 2011):

$$m_{C/C_0} = QC_0 \int_0^{t_{C/C_0}} \left(1 - \frac{C}{C_0}\right) dt \tag{3}$$

where m_{C/C_0} is mass of adsorbate (kg) at breakthrough time t_{C/C_0} (s); Q is gas flow rate (m^3/s); C_0 and C are the inlet and outlet IPA vapour concentrations (kg/m^3).

Equation (3) expresses dependence between C/C_0 and time using the Thomas equation (Srivastava et al. 2008):

$$\frac{C}{C_0} = \frac{1}{1 + \exp\left(\frac{k_{Th}q_{sat}m_{AC}}{Q} - C_0k_{Th}t\right)} \tag{4}$$

where k_{Th} is Thomas rate constant ($m^3kg^{-1}s^{-1}$), Q is the gas flow rate (m^3s^{-1}), q_{sat} is the adsorption capacity of activated carbon ($kg kg^{-1}$), m_{AC} is adsorbent mass (kg) and t is time (s).

The Thomas model is suitable for gas adsorption process with a constant flow rate. It employs the Langmuir isotherm and second-order reversible reaction kinetics. The model assumes plug-flow and neglects axial dispersion.

The calculate response breakthrough curve with parameters from Table 2 as the function of time are shown in Figs. 2 and 3. Equation parameters were determined with Statistica 10 software (StatSoft, Inc.) using the Levenberg-Marquardt method. A comparison of the Thomas model prediction to the experimental data also showed a good agreement between the inflection points and the shape of the curve. This is an indication that the model does correctly represent the IPA adsorption mechanisms on activated carbon. Therefore, the Thomas model can be applied for predicting the whole breakthrough curve. From such a curve, the adsorptive capacity of the adsorbent can be determined.

Table 2 The breakthrough curve parameters for IPA vapour adsorption process at 298 K

Cycle number	C_0 ($g m^{-3}$)	Q (m^3h^{-1})	$t_{5\%}$ (s)	TPR	LUB	K_{th} ($m^3kg^{-1}s^{-1}$)	q_{sat} ($kg kg^{-1}$)	R^2 (%)
C1	20.0	1.35	7,950	0.732	0.263	0.050	0.313	99.96
C2	16.6	1.40	8,790	0.700	0.310	0.047	0.312	99.97
C3	15.9	1.40	9,700	0.722	0.268	0.051	0.317	99.91
C5	14.6	1.40	10,120	0.729	0.280	0.052	0.303	99.93
C6	14.6	1.40	10,320	0.725	0.289	0.051	0.310	99.91
C14	15.5	1.60	9,250	0.728	0.313	0.052	0.339	99.96
C15	12.8	1.68	10,230	0.725	0.313	0.057	0.322	99.91
C21	15.0	2.07	7,920	0.717	0.301	0.056	0.366	99.92
C25	12.7	2.07	8,550	0.710	0.300	0.063	0.341	99.90
C41	12.8	2.08	8,850	0.703	0.300	0.059	0.361	99.95
C59	11.4	2.08	10,140	0.720	0.285	0.064	0.357	99.95
C60	11.8	2.05	8,740	0.703	0.293	0.060	0.355	99.86

Table 2 shows that the total adsorption capacity q_{sat} is dependent on input concentration and the efficiency of adsorbent regeneration in preceding cycles. The adsorption capacity of Sorbonorit 4 in cycle C1, was slightly different than that in successive cycles (C2–C3) when adsorbate inlet concentration was 17–20 % lower and adsorption occurred on regenerated adsorbent. It is probably the effect of initial heating of the virgin activated carbon bed prior to ETSA cyclic adsorption examination. The adverse effect of initial heating was also confirmed in vapour adsorption examination of other aliphatic alcohols on Sorbonorit 4 in ETSA system. Results are to be published in forthcoming papers.

A comparison of Sorbonorit 4 adsorption capacity values determined in BTC tests for the same inlet concentration values of the adsorbate shows that after 20 cycles adsorbent capacity was higher by 10–20 %, compared to preceding cycles. It depends on the regeneration degree of used adsorbent which affects BTC test outcomes in successive cycles. Changes in the adsorption capacity of activated carbon resistively heated are due to changes in the internal structure of Sorbonorit 4 and in the chemical composition of its surface. These findings were compared by adsorption equilibrium measurements by the gravimetric method and X-ray photoelectron spectroscopy examination. These are elaborated on at length below.

3.2 Adsorption isotherms of IPA

Figure 4 presents experimental adsorption isotherms of IPA vapours on three Sorbonorit 4 samples: virgin (sample S4), direct resistively heated (S4-ohm sample) and electrothermally regenerated (S4-reg sample).

Adsorption equilibrium measurements by the gravimetric method were conducted at 293 and 298 K in the range of

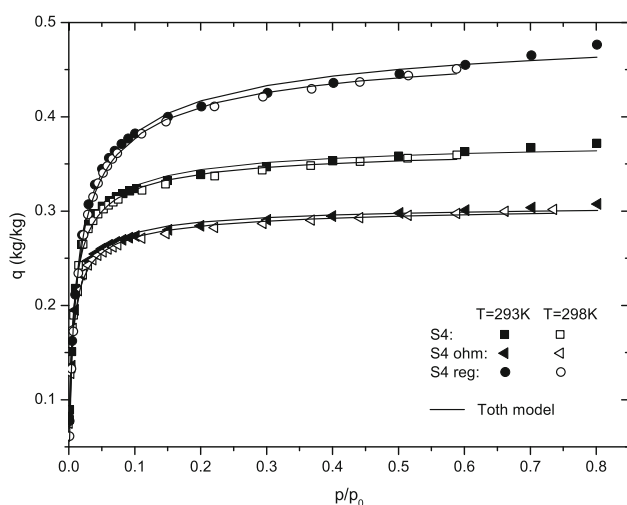


Fig. 4 Experimental adsorption isotherms of IPA vapours on Sorbonorit 4

relative pressure p/p_0 from 0.001 to 0.8, where p is the current pressure and p_0 is the saturated vapour pressure. In the analysed pressure range all adsorption isotherms are classified as Type I in the IUPAC scheme. This seems to suggest that mainly micropores are to be found in Sorbonorit 4 samples and IPA vapour adsorption occurs according to the micropore filling mechanism (Bansal and Goyal 2005). The shape of the initial part of adsorption isotherm depends on the adsorbent's heterogeneity and particularly on the content of surface oxygen groups that transform the surface nature of activated carbon from hydrophobic into hydrophilic (Bansal and Goyal 2005; Bradley and Rand 1995). During the initial adsorption stages, alcohol molecules mainly bind to oxygen surface groups (Bae and Do 2006).

Figure 4 demonstrates that S4-ohm sample had the lowest adsorption capacity in the whole p/p_0 range following direct resistive heat treatment of pure adsorbent at 423 K. Regenerated activated carbon has the highest adsorption capacity and its adsorption isotherm of IPA vapours is shifted towards higher adsorption levels. This means that its porous structure has changed following many cycles of carbon regeneration in ETSA process.

The knees of IPA adsorption isotherms of S4 and S4-ohm samples are sharper than that for the S4-reg sample, which means that narrower micropores in the former are filled in the first place (Bradley and Rand 1995). Within the region of medium and high relative pressures p/p_0 , the isotherms of S4 and S4-ohm gradually shift towards plateau and eventually reach the boundary adsorption values, i.e. the state when all pores are filled. This shape of isotherm is characteristic for adsorbents with poorly developed mesoporosity (Bae and Do 2006). The isotherm of IPA vapours on S4-reg carbon has a more rounded knee while in the region of high p/p_0 pressures it is a curve with a slight positive slope. This shape is evidence for a wider distribution of micropore sizes and for higher mesopore content compared to other samples (Branton and Bradley 2011).

Within the investigated range of IPA vapour pressures ($p/p_0 \leq 0.8$), we failed to observe hysteresis loop which would have confirmed that capillary condensation was taking place in wider pores.

The Toth model was used to describe adsorption equilibrium of IPA vapours on Sorbonorit 4 carbon samples (Kumar et al. 2011)

$$q = \frac{q_m p}{(b + p^t)^{1/t}} \quad (5)$$

where q is the amount adsorbed at equilibrium (kg kg^{-1}), q_m is the maximum adsorption capacity (kg kg^{-1}), b is a constant related to specific to adsorbate–adsorbent pairs (Pa^t) and t is the Toth isotherm exponent related to surface heterogeneity.

Table 3 Tòth equation parameters

Sample	293 K				298 K			
	q_m (kg kg ⁻¹)	b (Pa')	t	δ (%)	q_m (kg kg ⁻¹)	b (Pa')	t	δ (%)
S4	0.38	0.088	0.632	1.59	0.372	0.063	0.646	1.76
S4-ohm	0.309	0.084	0.702	1.69	0.309	0.101	0.610	1.77
S4-reg	0.513	0.064	0.532	1.04	0.490	0.032	0.600	1.23

The Tòth model provides a satisfactory description of IPA vapour adsorption in the whole investigated pressure range. Table 3 presents equation parameters determined with the nonlinear regression method using Statistica 10 software. The goodness-of-fit of a model to data was evaluated on the basis of average relative error:

$$\delta = \frac{1}{N} \sum_{i=1}^N \left| \frac{q_{exp} - q_{mod}}{q_{exp}} \right| \tag{6}$$

where q_{exp} is the experimental adsorption capacity, q_{mod} is the calculated adsorption capacity, and N is the number of experimental points.

The values of average relative error δ demonstrate similar agreement of both temperatures. The values of t exponent in the Tòth isotherm equation ($t < 1$) indicate that the examined activated carbons are heterogeneous (Kumar et al. 2011).

A comparison of adsorption capacity q and q_{sat} at 298 K for the same adsorbate inlet concentrations calculated with the Tòth and Thomas models (Tables 4 and 2, respectively) shows that Tòth isotherm for S4 sample provides the best fit for cycles C2–C20, while the isotherm for S4-reg for cycles C21–C60.

For S4-ohm sample, the Tòth equation yields underestimated values of adsorption capacity for all adsorption cycles, including cycle C1. Hence, eight cycles of resistive heating of pure Sorbonorit 4 led to a more substantial lowering of adsorbent capacity than one individual cycle of bed heating prior to cycle C1.

3.3 Characterisation of pore structure

The Dubinin–Radushkevich (DR) equation is widely used for determination of microporous structure in homogenous activated carbons (Nguyen and Do 2001):

$$W = W_0 \exp \left[\left(\frac{RT}{E} \right)^2 \ln^2 \left(\frac{p_0}{p} \right) \right] \tag{7}$$

where W is the volume of adsorbate in the unit mass of adsorbent (cm³g⁻¹), W_0 is limiting micropore volume (cm³g⁻¹), E is the characteristic energy of the adsorption system (J mol⁻¹), T is absolute temperature (K), p is the pressure in the gas phase, p_0 is the IPA saturation vapour

Table 4 Adsorption capacity of IPA on Sorbonorit 4 samples

C_0 (g m ⁻³)	q (kg kg ⁻¹)		
	S4	S4-reg	S4-ohm
12.8	0.319	0.370	0.269
15.0	0.323	0.378	0.273
16.0	0.325	0.382	0.274
20.0	0.331	0.393	0.278

pressure at temperature T , R is ideal gas constant (8.314J mol⁻¹ K⁻¹).

The values of DR micropore volume W at relative pressure p/p_0 were calculated as the product of liquid molar volume of IPA at 293 K and experimental concentrations of adsorbate q (mol kg⁻¹). In order to determine the parameters of the DR equation, its linear form can be used:

$$\ln W = \ln W_0 + \left(\frac{RT}{E} \right)^2 \ln^2 \left(\frac{p_0}{p} \right) \tag{8}$$

Figure 5 presents curves of $\ln W$ in relation to $\ln^2(p_0/p)$ for IPA vapour adsorption on Sorbonorit 4 samples. The curves are linear in narrow pressure ranges p/p_0 . In the pressure range of $p/p_0 > 0.4$ (low values of $\ln^2(p_0/p)$) all the curves deviate from type C linearity, according to the Marsh–Rand classification (Bradley and Rand 1995). Such deviations are characteristic for adsorption in pores larger than micropores. In the pressure range of $p/p_0 < 0.1$, the curves of all samples display nonlinear deviation of type A which is characteristic for adsorbends with a wide distribution of micropore sizes (Bradley and Rand 1995).

The shape of characteristic curves for $\ln W$ in relation to $\ln^2(p_0/p)$ indicates heterogeneity of the internal structure in the investigated carbons, formed by pores of various sizes. The structural heterogeneity of fresh Sorbonorit 4 is confirmed by results of pore size distribution analysis using the Barrett–Joyner–Halend method (BJH) from nitrogen adsorption isotherm at 77 K, presented elsewhere (Kavitha 2010). Analysis shows that in the range of 1–50 nm, fresh Sorbonorit 4 contains three groups of pores: micropores (1.2–1.4 nm in size), supermicropores (1.4–3 nm) and mesopores (3–50 nm). Such pore size distribution is

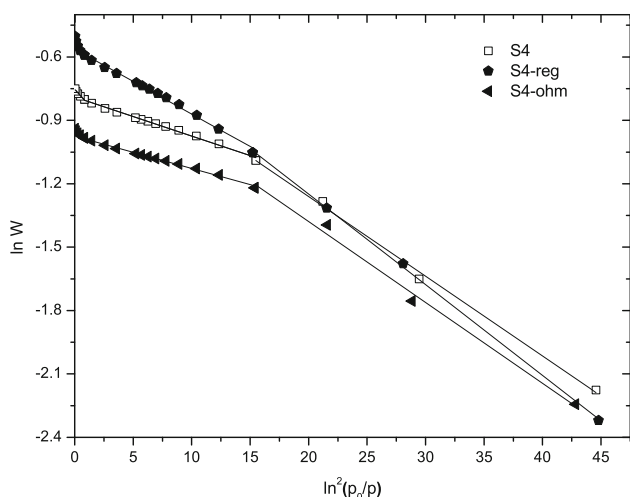


Fig. 5 IPA characteristic adsorption curves for Sorbonorit 4

characteristic for steam activated carbons (Bansal and Goyal 2005).

A modified Dubinin–Astakhov equation (D–A) was used to describe IPA vapour adsorption on structurally heterogeneous adsorbents (Gil and Grange 1996):

$$\theta = \frac{W}{W_0} = \sum_i f_i \exp \left[- \left(\frac{A}{E_i} \right)^n \right] \quad (9)$$

where θ is the relative adsorption, defined as the ratio of the amount adsorbed in micropores W to the limiting micropore adsorption capacity W_0 , A is adsorption potential, defined as $A = RT \ln(p_0/p)$, f_i denotes the fraction of adsorption sites located in micropores with an adsorption characteristic energy E_i , exponent n , is a measure of the heterogeneity of the adsorbent-adsorbate system.

Equation (9) is based on the assumption that an adsorbent possesses micropores of the same shape but different sizes. The concentration of a micropore group can be calculated from Equation (Gil and Grange 1996):

$$f_i = \frac{W_{0i}}{W_0} \quad (10)$$

where W_0 is the total micropore volume defined as the sum of volumes of successive micropore fractions W_{0i} :

$$W_0 = \sum_i W_{0i} \quad (11)$$

The parameters W_{0i} and E_i were calculated from slopes $(RT/E_i)^n$ and intercepts $\ln(W_{0i})$ of linear sections of $\ln(W)$ in relation to A^n by means of the least squares method. The values of exponent n were selected from the range of 1–4 (Carrasco-Marin et al. 1996) to obtain the best fit of experimental and calculated results. The calculations were conducted in the range of relative pressures $p/p_0 \leq 0.4$ which satisfy the formal conditions of D–A equation.

Table 5 presents the parameter values of Eq. (9) for IPA-Sorbonorit 4 systems and total volumes of adsorbate W_t determined experimentally for the relative pressure $p/p_0 = 0.8$ at 293 K. A comparison of W_t values shows that the adsorption capacity of S4-ohm sample is lower by 17 % than that of S4 sample. By contrast, the capacity of S4-reg sample is greater by 28 %.

Data from Table 5 indicate that adsorption of IPA vapours on S4 and S4-ohm samples occurs following the filling of two micropore fractions. Initially, at low pressure values p/p_0 ($0.002 < p/p_0 < 0.1$), adsorption in narrow micropores with volume W_{01} and characteristics adsorption energy E_1 is observed. Micropores with energy E_2 are filled in the region of higher pressures p/p_0 . Consequently, both adsorbents have a bimodal structure with dominating narrower micropores. High values of adsorption fields of opposite walls in narrow micropores (Bradley and Rand 1995).

The adsorption energy E_1 in S4 and S4-ohm samples is about 3.5 times larger than energy E_2 characterising the fraction of wider micropores. S4-reg carbon contains only one fraction of micropores with the lowest energy E_1 out of all the examined carbon samples. The values of exponent n for S4-reg sample is within the range $2 < n < 3$, which is typical for activated carbons with relatively homogeneous micropores (Bansal and Goyal 2005). Values $n > 3$ (S4 and S4-ohm samples) are characteristic for adsorbents with narrow micropores of small size range (Erdem-Şenatalar et al. 2000).

The difference between the total micropore volume W_t and specific micropore value W_0 (Table 5) shows that each analysed carbon contains mesopores which are filled at higher pressures of IPA vapours. 2 % (S4-ohm sample), 4 % (S4 sample) and 8 % (S4-reg sample) of total adsorbate is adsorbed in such pores for the relative pressure $p/p_0 = 0.8$.

3.4 Chemical structure of the activated carbon surface

Adsorption properties of activated carbon depend both on its porous structure (shape, pore size and volume) and on the chemistry of its surface. The surface groups are bonded to the edges and corners of the aromatic sheets (Bansal and Goyal 2005). The behaviour of carbon surface and its functional groups depends on the size and shape of sheets, the presence and location of other groups and π -electrons. XPS spectra provide data about the elemental composition of the outer layers of activated carbon (the analysis depth is about 10^{-12} nm). Figure 6 presents wide scan spectra in the binding energy range of 0–1,400 eV for all Sorbonorit 4 samples. The spectra were used to identify elements in narrow energy regions. Interpretation of XPS spectra is based on binding energies (BE) from reference compounds. For all the samples, spectra consist of two independent

Table 5 Tòth equation parameters

Sample	Equation (9)							
	W_t (cm ³ g ⁻¹)	n	W_{01} (cm ³ g ⁻¹)	W_{02} (cm ³ g ⁻¹)	W_0 (cm ³ g ⁻¹)	E_1 (kJmol ⁻¹)	E_2 (kJmol ⁻¹)	δ (%)
S4	0.473	3.6	0.415	0.039	0.454	14.37	4.28	1.38
S4-ohm	0.391	3.7	0.354	0.028	0.382	15.41	4.42	2.23
S4-reg	0.606	2.4	0.56	–	0.56	13.16	–	1.29

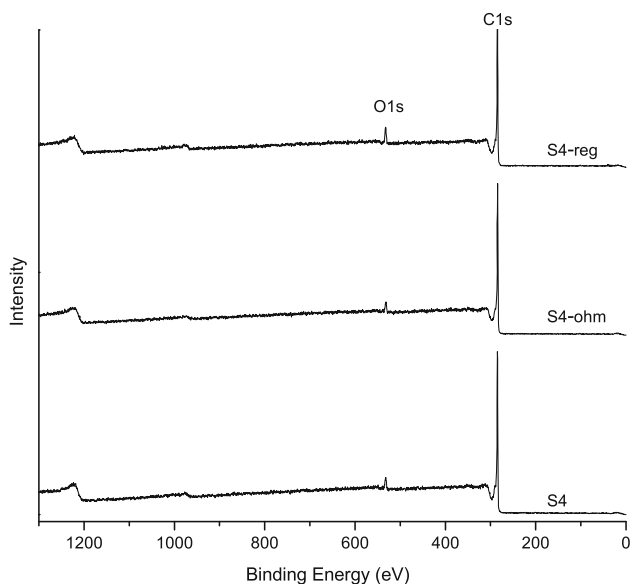


Fig. 6 Wide scan XPS spectra of activated carbon samples

peaks, C1s at 285 eV and O1s at 532 eV. Narrow scan spectra C1s in the region of 285 eV (Fig. 7) and O1s at 535.5 eV (Fig. 8) were used for quantitative analysis of the elemental surface composition of Sorbonorit 4 samples and to identify the chemical states of both elements.

Data in Table 6 shows that elemental carbon is the main component in the surface of the analysed activated carbon. Its concentration ranges from 93 to 96 %. The O/C ratio shows that the degree of carbon surface oxidation decreases as a result of resistive heating in inert atmosphere (S4-ohm sample) and increases following electrothermal regeneration (S4-reg sample). Similar changes affecting the degree of surface oxidation were reported in literature (Hashisho et al. 2005; Tazibet et al. 2014).

A broad asymmetric shape (Fig. 7) extending from 282 to 294 eV indicates the presence of several carbon species of different binding energies (Lee and Reucroft 1999). The maximum of C1s peak for S4-reg sample is lower relative to other peaks. It means that the chemical state of carbon surface was changed following cyclic adsorption. In order to identify specific surface carbon groups, C1s spectra were deconvoluted into components using CasaXPS software. Then, relative concentration of all functional groups were

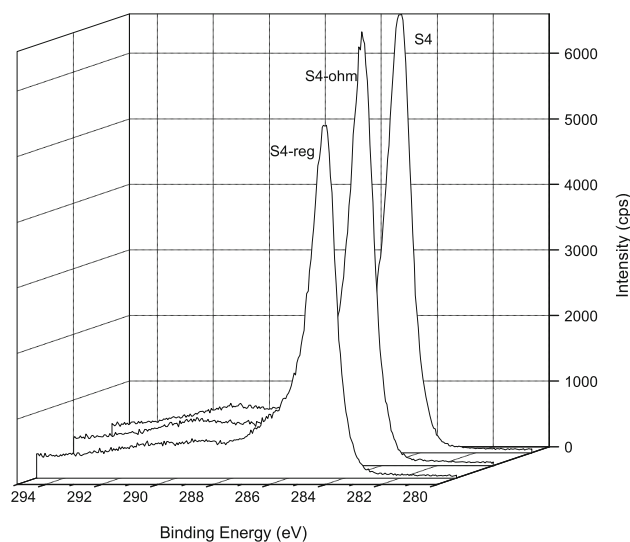


Fig. 7 Carbon 1s narrow XPS spectra of activated carbon samples

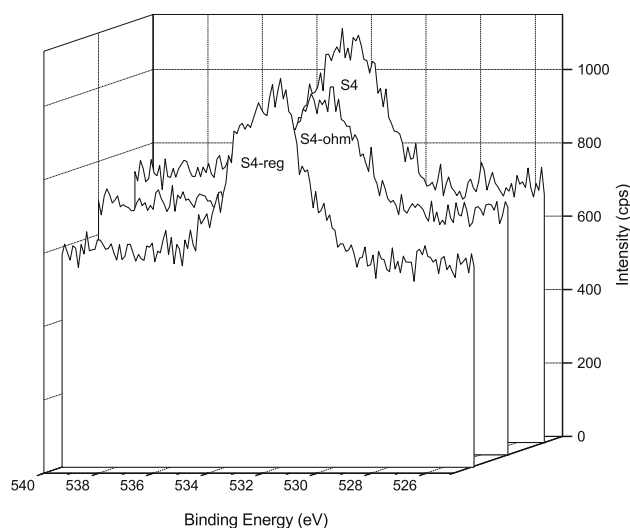


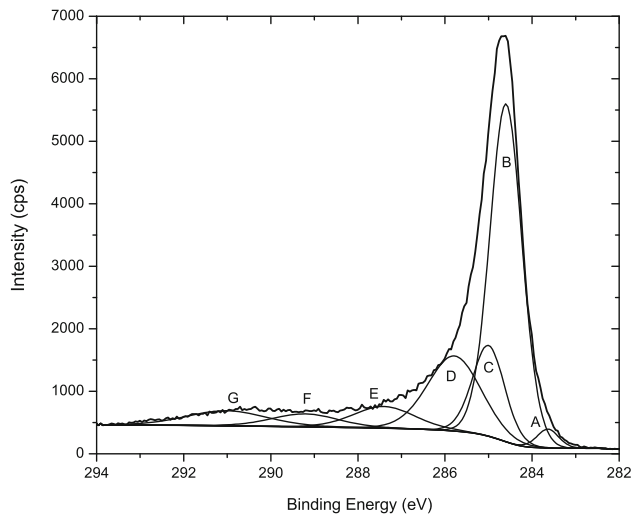
Fig. 8 Oxygen 1s narrow XPS spectra of activated carbons

calculated based on peak areas. An iterative least-squares fitting algorithm was used to decompose XPS peaks, the curves being taken as 30 % Gaussian and 70 % Lorentzian.

Figure 9 presents an example of C1s spectrum for pure Sorbonorit 4 deconvoluted into functional group

Table 6 Activated carbon surface elemental composition obtained by XPS analysis

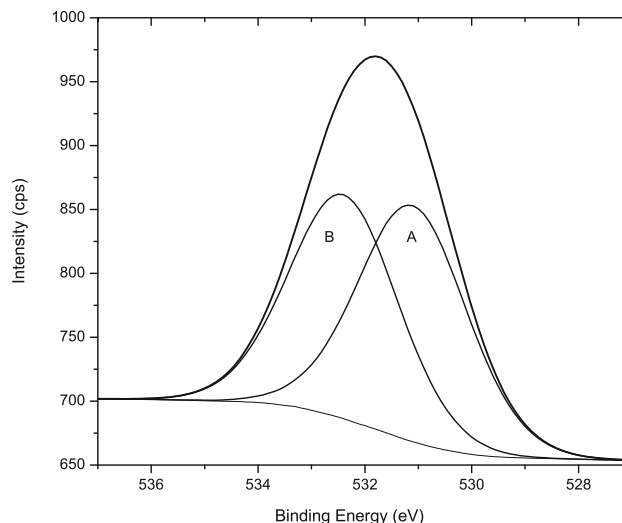
Sample	Atomic concentration (wt%)		O/C ratio
	Carbon (C)	Oxygen (O)	
S4	95.58	4.42	0.046
S4-ohm	96.31	3.68	0.038
S4-reg	93.02	6.16	0.066

**Fig. 9** XPS spectra of C1s on Sorbonorit 4 sample surfaces

contributions. As a result of deconvolution of C1s spectrum, seven constituent peaks were obtained with the following BE values: 283.7, 284.6, 285, 286.6, 287.2, 289.1 and 291 eV. Based on BE values, the following components were identified: aromatic carbon (peak B), aliphatic carbon (peak C), functional carbon atoms present in hydroxyl groups of phenolic character (peak D), carbonyl (peak E) and carboxyl groups (peak F). The most intensive peak in C1s spectrum represents aromatic carbon, belonging to graphite-like domains with hexagonal carbon rings. The satellite peak at 290.5 eV is induced by a cloud of π -electrons observed in activated carbon.

Deconvolution of O1s spectrum (Fig. 10) demonstrated the presence of two oxygen group contributions with the binding energy of 531.6 eV (A peak) and 532.9 eV (B peak). The A peak with lower binding energy is associated with oxygen doubly bound to carbon (C=O in carbonyl or carboxyl groups). The B peak corresponds to oxygen with a single bond to carbon (C–O in alcohol groups).

Table 7 presents the values of binding energy and relative content of functional groups for all carbon samples. Relative content of oxygen was defined as the sum of atomic contributions in oxygen functional groups (Chiang and Chen 2010). The chemical composition of the surface of virgin activated carbon (S4 sample) depends on the type

**Fig. 10** XPS spectra of O1s on Sorbonorit 4 sample surfaces

of precursor activating agent (steam), carbonisation and activation conditions (Bansal and Goyal 2005). Table 7 shows that non-functionalised carbons (aromatic and aliphatic carbons) are the main surface components of Sorbonorit 4 carbons. For virgin carbon (S4 sample), they make up 61 % of the total area of C1s peak region, with dominating aromatic carbons (aliphatic/aromatic carbon ratio of 27 %). As a result of resistive heating in inert atmosphere at 423 K (S4-ohm sample) the content of non-functionalised carbons dropped to 54 % and the aliphatic to aromatic carbon ratio fell to 24 %. As a result of electrothermal regeneration (S4-reg sample) the content of aliphatic carbons increased due partial decomposition of aromatic rings (aliphatic/aromatic carbon ratio of 35 %). The percentage share of non-functionalised carbons is comparable with S4-ohm sample. Following concentration changes in hydrocarbon groups, the concentration of π -electrons which are voltage carriers also changes. The highest intensities of the π - π^* transitions in aromatic rings were recorded for S4-ohm and the lowest for S4-reg. An increase of carbon S4-reg surface oxidation is the cause of the impoverishment of π -electron binding in aromatic sheets (Chiang and Chen 2010; Daud and Houshamnd 2010).

All oxygen functional groups identified on the surface of Sorbonorit 4 samples (Table 7) are acidic groups (Bansal and Goyal 2005). The groups are present mainly at the edges and corners of the aromatic sheets. Resistive heating of Sorbonorit 4 (S4-ohm sample) results in a substantial increase of the content of hydroxyl surface groups. The groups play the role of primary active centres. Adsorbed alcohol molecules bind to them and form clusters located in the vicinity of micropore internal structures (Agnihotri et al. 2005; Tamon and Okazaki 1996). A substantial

Table 7 Deconvolution of C1s and O1s peak areas into functional groups for Sorbonorit 4 samples

Region	Peak	Binding energy (eV)	Surface functional groups	Percentage of total area peaks		
				S4	S4-ohm	S4-reg
C1s	A	283.7 ± 0.1		1.81	1.97	2.64
	B	284.6 ± 0.1	Aromatic carbon (C-(C, H))	48.15	43.42	41.25
	C	285.0 ± 0.1	Aliphatic carbon (C-(C, H))	12.95	10.43	14.42
	D	285.6 ± 0.1	Alcohol carbon (C-OH)	17.67	24.99	13.6
	E	287.2 ± 0.1	Carbonyl carbon (C=O)	5.85	5.91	11.86
	F	289.1 ± 0.1	Carboxyl carbon (COOH)	3.82	3.28	5.23
	G	291.0 ± 0.1	Shake-up band, ($\pi \rightarrow \pi^*$)	5.33	5.33	4.02
O1s	A	531.6 ± 0.3	(=O) in carbonyl, carboxyl groups	2.53	1.89	3.73
	B	532.9 ± 0.3	(-O-) in phenolic hydroxyl groups	1.89	1.79	2.43

concentration of C–OH groups on the surface of S4-ohm sample is the reason for lower adsorption capacity of IPA vapours compared to S4 sample (Chiang and Chen 2010). The surface of regenerated Sorbonorit 4 contains the fewest number of hydroxyl groups and the highest number of groups with double bonds, such as carbonyl and carboxyl groups. Such chemical composition of activated carbon surface improves its adsorption properties resulting in increased adsorption of IPA vapours. Evidence for the fact is to be found in measurement results of adsorption equilibria presented in Sect. 3.2. As regeneration of Sorbonorit 4 via a direct resistive method, it enables effective capture of IPA vapours in air in a cyclic ETSA process.

4 Conclusions

The adsorption properties of an adsorbate–adsorbent system determine its performance in a cyclic ETSA process. The process involves the use of activated carbon which conducts electrical current. The electrical characteristics of the adsorbent must enable the effective regeneration using the direct resistive heating. The requirements are fulfilled by some types of granular activated carbon, activated carbon monolith and ACFC.

The paper presented the influence of direct resistive heating on the adsorption properties of Sorbonorit 4 activated carbon used for the adsorption of IPA vapours in an ETSA process. BTC tests in ETSA system showed that the adsorption efficiency of IPA vapours on Sorbonorit 4 is dependent on adsorbate input concentration, purified gas flow rate and the degree of adsorbent regeneration in a preceding adsorption cycle. Improperly selected operation parameters of electrothermal desorption and too limited duration of the process lead to a shortened service life of a fixed-bed at the adsorption phase in a successive ETSA

cycle. The Thomas model well fitted the experimental breakthrough curves for IPA vapours on Sorbonorit 4. Its maximum adsorption capacity values determined in BTC tests indicate that the adsorption capacity of activated carbon increases following multiple cycles of electrothermal regeneration.

The nature of electrothermally-induced changes in the internal structure of Sorbonorit 4 and in the chemical composition of its surface were assessed based on adsorption equilibrium measurements by the gravimetric and XPS methods. Three samples of virgin, resistively heated and electrothermally regenerated Sorbonorit 4 were used. Adsorption isotherm model demonstrated that Sorbonorit 4 is a heterogeneous adsorbent and that the Tòth equation provides a good agreement with experimental data.

The structural characteristics of activated carbon determined with a modified Dubinin–Astakhov equation show that pure and resistive heated Sorbonorit 4 has a bimodal structure, formed by two micropore fractions, with the energetic fraction being the dominant one while regenerated Sorbonorit 4 contains only one fraction of micropores. XPS analysis revealed that the same hydroxyl, carbonyl and carboxyl groups were found on the surface of all Sorbonorit 4 samples, albeit in different volume ratios. As a result of direct resistive heating, the adsorption capacity of Sorbonorit 4 decreased by approximately 18 % compared to that of pure carbon. The equilibrium adsorption capacity of regenerated Sorbonorit 4 is by approximately 20 % higher than that of pure carbon owing to electrothermal heating-induced structural changes and altered surface chemistry.

Open Access This article is distributed under the terms of the Creative Commons Attribution License which permits any use, distribution, and reproduction in any medium, provided the original author(s) and the source are credited.

References

- Agnihotri, S., Rood, M.J., Rostam-Abad, M.: Adsorption equilibrium of organic vapors on single-walled carbon nanotubes. *Carbon* **43**, 2379–2388 (2005)
- Ania, C.O., Menéndez, J.A., Parra, J.B., Pis, J.J.: Microwave-induced regeneration of activated carbons polluted with phenol. A comparison with conventional thermal regeneration. *Carbon* **42**, 1383–1387 (2004)
- Bae, J.S., Do, D.D.: On the equilibrium and dynamic behavior of alcohol vapors in activated carbon. *Chem. Eng. Sci.* **61**, 6468–6477 (2006)
- Bansal, R., Goyal, M.: *Activated Carbon Adsorption*. CRC Press, Boca Raton (2005)
- Bradley, R.H., Rand, B.: On the physical adsorption of vapors by microporous carbons. *J. Colloid Interface Sci.* **169**, 168–176 (1995)
- Branton, P., Bradley, R.H.: Effects of active carbon pore size distributions on adsorption of toxic organic compounds. *Adsorption* **17**, 293–301 (2011)
- Carrasco-Marin, F., Alvarez-Merino, M.A., Moreno-Castilla, C.: Microporous activated carbons from a bituminous coal. *Fuel* **75**, 966–970 (1996)
- Celzard, A., Maréché, J.F., Payot, F., Bégin, D., Furdin, G.: Electrical conductivity of anthracites as a function of heat treatment temperature. *Carbon* **38**, 1207–1215 (2000)
- Chiang, Y.C., Chen, T.C.: Surface characterization and adsorption performance of electrochemically oxidized activated carbon fibers. *J. Environ. Eng. Manag.* **20**, 387–395 (2010)
- Coss, P.M., Cha, C.Y.: Microwave regeneration of activated carbon used for removal of solvents from vented air. *J. Air Waste Manag. Assoc.* **50**, 529–35 (2000)
- Daud, W.M.A.W., Houshamnd, A.: Textural characteristics, surface chemistry and oxidation of activated carbon. *J. Nat. Gas Chem.* **19**, 267–279 (2010)
- Downarowicz, D.: Evaluation of the isopropanol vapour desorption efficiency of ETSA process. *Inż. Ap. Chem.* **45**, 37–38 (2006)
- Downarowicz, D., Gabruś, E.: Electrothermal temperature swing adsorption: a chance of effective voc recovery from flue gases. *Przem. Chem.* **87**, 768–774 (2008)
- Downarowicz, D., Nastaj, J.: Improvement efficiency of electrothermal activated carbon heating: application to desorption process. In: Conference proceedings of the Chisa'2002, Praha, Czech Republic, CD-ROM P3.159, pp. 1–12 (2002)
- Erdem-Şenatalar, A., Tatler, M., Sirkecioğlu, A.: The relationship of the geometric factor in the Dubinin-Astakhov isotherm equation with the fractal dimension. *Colloids Surf. A* **173**, 51–59 (2000)
- Figueiredo, J., Pereira, M.F.R., Freitas, M.M.A., Órfão, J.: Modification of the surface chemistry of activated carbons. *Carbon* **37**, 1379–1389 (1999)
- Fletcher, A.J., Yüzak, Y., Thomas, K.M.: Adsorption and desorption kinetics for hydrophilic and hydrophobic vapors on activated carbon. *Carbon* **44**, 989–1004 (2006)
- Gil, A., Grange, P.: Application of the Dubinin-Radushkevich and Dubinin-Astakhov equations in the characterization of microporous solids. *Colloids Surf. A* **113**, 39–50 (1996)
- Grande, C.A., Ribeiro, R.P.L., Oliveira, E.L.G., Rodrigues, A.E.: Electric swing adsorption as emerging CO₂ capture technique. *Energy Procedia* **1**, 1219–1225 (2009)
- Gu, J., Faqir, N.M., Bart, H.J.: Drying of an activated carbon column after steam regeneration. *Chem. Eng. Technol.* **22**, 859–864 (1999)
- Hashisho, Z., Rood, M.J., Barot, S., Bernhard, J.: Role of functional groups on the microwave attenuation and electric resistivity of activated carbon fiber cloth. *Carbon* **47**, 1814–1823 (2009)
- Hashisho, Z., Rood, M.J., Botich, L.: Microwave-swing adsorption to capture and recover vapors from air streams with activated carbon fiber cloth. *Environ. Sci. Technol.* **39**, 6851–6859 (2005)
- Jou, C.J.G., Wu, C.R., Lee, C.L.: Application of microwave energy to treat granular activated carbon contaminated with chlorobenzene. *Environ. Prog. Sustain. Energy* **29**, 272–277 (2010)
- Kavitha, T.: Equilibrium and kinetic studies of biogas adsorption onto porous solids. PhD dissertation, Anna University Chennai India, Faculty of Civil Engineering (2010)
- Kumar, K.V., de Castro, M.M., Martinez-Escandell, M., Molina-Sabio, M., Rodriguez-Reinoso, F.: A site energy distribution function from Toth isotherm for adsorption of gases on heterogeneous surfaces. *Phys. Chem. Chem. Phys.* **13**, 5753–5759 (2011)
- Lee, W.H., Reucroft, P.J.: Vapor adsorption on coal- and wood-based chemically activated carbons (II) adsorption of organic vapors. *Carbon* **37**, 15–20 (1999)
- Li, X., Li, Z.: Adsorption of water vapor onto and its electrothermal desorption from activated carbons with different electric conductivities. *Sep. Purif. Technol.* **85**, 77–82 (2012)
- Luo, L., Ramirez, D., Rood, M.J., Grevillot, G., Hay, K.J., Thurston, D.L.: Adsorption and electrothermal desorption of organic vapors using activated carbon adsorbents with novel morphologies. *Carbon* **44**, 2715–2723 (2006)
- Nastaj, J., Aleksandrak, T.: Adsorption isotherms of water, propan-2-ol, and methylbenzene vapors on Grade 03 silica gel, Sorbonorit 4 activated carbon, and Hisiv3000 zeolite. *J. Chem. Eng. Data* **58**, 2629–2641 (2013)
- Nguyen, C., Do, D.: The Dubinin-Radushkevich equation and the underlying microscopic adsorption description. *Carbon* **39**, 1327–1336 (2001)
- Paderewski, M., Downarowicz, D.: Study on possibilities of regeneration of active carbon by direct resistance heating. *Przem. Chem.* **81**, 391–394 (2002)
- Petkovska, M., Antov-Bozalo, D., Markovic, A., Sullivan, P.D.: Multiphysics modeling of electric-swing adsorption system with in-vessel condensation. *Adsorption* **13**, 357–372 (2007)
- Ramirez, D., Emamipour, H., Vidal, E.X., Rood, M.J., Hay, K.J.: Capture and recovery of methyl ethyl ketone with electrothermal-swing adsorption systems. *J. Environ. Eng.* **137**, 826–832 (2011)
- Rodriguez-Reinoso, F.: Role of carbon materials in heterogeneous catalysis. *Carbon* **36**, 159–175 (1998)
- Shen, W., Li, Z., Liu, Y.: Surface chemical functional groups modification of porous carbon. *Recent Pat. Chem. Eng.* **1**, 27–40 (2008)
- Srivastava, V.C., Prasad, B., Mishra, I.M., Mall, I.D., Swamy, M.M.: Prediction of breakthrough curves for sorptive removal of phenol by bagasse fly ash packed bed. *Ind. Eng. Chem. Res.* **47**, 1603–1613 (2008)
- Sullivan, P.D., Rood, M.J., Dombrowski, K.D., Hay, K.J.: Capture of organic vapors using adsorption and electrothermal regeneration. *J. Environ. Eng.* **130**, 258–267 (2004)
- Tamon, H., Okazaki, M.: Influence of acidic surface oxides of activated carbon on gas adsorption characteristics. *Carbon* **34**, 741–746 (1996)
- Tazibet, S., Lodewyckx, P., Boucheffa, Y.: The influence of the cooling down step in the heat treatment on the stability of activated carbons hydrophobicity. *Adsorption* **20**, 545–553 (2014)
- Yaws, C.L.: *Yaws' Handbook of Thermodynamic and Physical Properties of Chemical Compounds*. Knovel, New York (2003)